J|A|C|S
ARTICLES

Metal-Catalyzed Simultaneous Chain- and Step-Growth Radical Polymerization: Marriage of Vinyl Polymers and Polyesters

Masato Mizutani, Kotaro Satoh, and Masami Kamigaito*

Department of Applied Chemistry, Graduate School of Engineering, Nagoya University, Furo-cho, Chikusa-ku, Nagoya 464-8603, Japan

Received March 22, 2010; E-mail: kamigait@apchem.nagoya-u.ac.jp

Abstract: All polymerization reactions are categorized into two large different families, chain- and step-growth polymerizations, which are typically incompatible. Here, we report the simultaneous chain- and step-growth polymerization via the metal-catalyzed radical copolymerization of conjugated vinyl monomers and designed monomers possessing unconjugated C═C and active C−Cl bonds. Especially, almost ideal linear random copolymers containing both vinyl polymer and polyester units in a single polymer chain were formed by the CuCl/1,1,4,7,10,10-hexamethyltriethylenetetramine- or RuCp*Cl(PPh_3)$_2$-catalyzed copolymerization of methyl acrylate (MA) for the chain-growth polymerization and 3-butenyl 2-chloropropionate (**1**) for the step-growth polymerization. In contrast, other transition metal catalysts, such as CuCl with tris[2-(dimethylamino)ethyl]amine or *N*,*N*,*N*′,*N*′′,*N*′′-pentamethyldiethylenetriamine and $FeCl_2$/P*n*Bu_3, resulted in branched structures via the concomitant chain-growth copolymerization of **1** with MA. The polymerization mechanism was studied in detail by NMR and MALDI-TOF-MS analyses of the polymerizations as well as the model reactions. Furthermore, a series of copolymers changing from random to multiblock polymer structures were obtained by varying the feed ratios of the two monomers. These copolymers can be easily degraded into lower molecular weight oligomers or polymers via methanolysis of the ester-linkages in the main chain using sodium carbonate.

Introduction

All synthetic polymers such as polystyrenes, acrylic polymers, polyesters, polyamides, and so forth, which heavily support our modern life, are obtained by either a chain- or step-growth polymerization. These two classes of polymerizations are mechanistically completely different and proceed via their characteristic profiles of polymer chain propagation to produce the polymers with their unique structures.[1] In the chain-growth mechanism, polymer chains grow via reactions of the growing chain end with monomers, while in the step-growth counterpart, the chain gradually propagates via reactions among the functional chain-end groups of the monomer, oligomers, and finally polymers. The former representatives are radical polymerizations of vinyl monomers, which produce C−C bond main-chain polymers, whereas the latter includes polycondensation for polyesters and polyaddition for polyurethane, mostly containing heteroatoms in the main chains. If one could simultaneously perform both the chain- and step-growth polymerizations, the accessible polymer structures and properties could be widely varied. However, these two polymerizations are generally incompatible, and no such systems have been reported.[2]

The metal-catalyzed atom transfer or Kharasch radical addition reaction[3,4] is one of the most highly efficient and robust carbon−carbon bond forming reactions between various vinyl compounds and organic halides.[5−11] This reaction has now quite successfully been developed into chain-growth radical polymerizations of mostly conjugated various vinyl monomers in the presence of an appropriate organic halide initiator to establish a new category of precision polymerizations, that is, the metal-catalyzed living radical polymerization or atom transfer radical polymerization (ATRP).[12−25] In contrast, we quite recently developed the radical addition reaction into step-growth polymerizations, that is, the metal-catalyzed radical polyaddition of designed monomers (C═C-R-C-X) with active carbon−halogen and unconjugated C═C double bonds.[26−30] The common process of both polymerizations lies in the metal-assisted formation of carbon-centered radical species from the active C−X bond followed by the addition to the C═C double bond and the formation of a new C−X bond. However, the differences in the reactivity[22] of the newly formed C−X bond determine

---

(1) Odian, G. *Principles of Polymerization*, 4th ed.; John Wiley and Sons, Inc.: Hoboken, NJ, 2004.
(2) Yokozawa, T.; Yokoyama, A. *Chem. Rev.* **2009**, *109*, 5595–5619.
(3) Kharasch, M. S.; Jensen, E. V.; Urry, W. H. *Science* **1945**, *102*, 128–128.
(4) Kharasch, M. S.; Urry, W. H. *J. Am. Chem. Soc.* **1945**, *67*, 1626–1626.
(5) Minisci, F. *Acc. Chem. Res.* **1975**, *8*, 165–171.
(6) Iqbal, J.; Bhatia, B.; Nayyar, N. K. *Chem. Rev.* **1994**, *94*, 519–564.
(7) Gossage, R. A.; van de Luil, L. A.; van Koten, G. *Acc. Chem. Res.* **1998**, *31*, 423–431.
(8) Nagashima, H. In *Ruthenium in Organic Synthesis*; Murahashi, S.-I., Ed.; Wiley-VCH: Weinheim, 2004; pp 333−343.
(9) Delaude, L.; Demonceau, A.; Noels, A. F. *Top. Organomet. Chem.* **2004**, *11*, 155–171.
(10) Pintauer, T.; Matyjaszewski, K. *Chem. Soc. Rev.* **2008**, *37*, 1087–1097.
(11) Fernández-Zúmel, M. A.; Thommes, K.; Kiefer, G.; Sienkiewicz, A.; Pierzchala, K.; Severin, K. *Chem.—Eur. J.* **2009**, *15*, 11601–11607.

10.1021/ja1023892

Scheme 1. Mechanism of Metal-Catalyzed Simultaneous Chain- and Step-Growth Radical Polymerization[a]

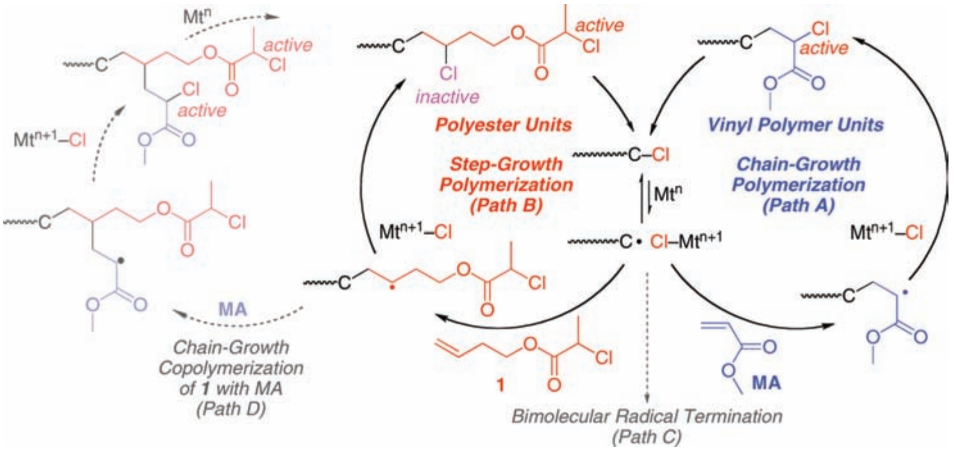

[a] Path A: chain-growth radical polymerization of MA. Path B: step-growth radical polymerization of **1**. Path C: possible bimolecular radical termination. Path D: possible chain-growth radical copolymerization of **1** with MA.

the reaction pathway. In the metal-catalyzed living radical polymerizations, the C−X bond, which is adjacent to the conjugated carbonyl or aryl groups originating from the conjugated vinyl monomers, can be repeatedly activated by a metal catalyst with moderate activity to reversibly form the growing radical species and to induce the chain-growth propagation. In contrast, in the radical polyaddition, the newly formed C−X bond derived from the unconjugated C═C double bond is hardly activated by the usual metal catalyst, while the original active C−X bond at the monomer, oligomer, and polymer terminals is selectively activated to induce the step-growth radical polymerizations.

We now report the unprecedented simultaneous chain- and step-growth polymerizations, both of which proceed via the radical intermediate generated by the same metal catalyst, for the synthesis of novel polymer structures with varying random to multiblock copolymers consisting of vinyl and polyester monomer units (Scheme 1). A series of transition metal catalysts (Cu, Ru, and Fe) with various ligands, which are effective for the metal-catalyzed living radial polymerization or ATRP, were extensively tested under various conditions to achieve the ideal simultaneous polymerizations of methyl acrylate (MA) and 3-butenyl 2-chloropropionate [CH_2═$CHCH_2CH_2OC(O)$-$CH(CH_3)Cl$: **1**]. One of the most important keys to the efficient simultaneous polymerizations resulting in the linear copolymers is to reduce any possible side reactions, such as the bimolecular radical termination and chain-growth copolymerization of **1** with MA. Detailed analyses of the polymerizations as well as the model reactions by NMR and MALDI-TOF-MS were thus done systematically to find the most efficient catalysts and to reveal the polymerization mechanism. Among the various metal catalysts, CuCl/1,1,4,7,10,10-hexamethyltriethylenetetramine (HMTETA) and RuCp*Cl(PPh_3)$_2$ proved most effective for the ideal simultaneous chain- and step-growth radical polymerizations to yield the linear copolymers comprised of acrylate and polyester monomer units.

Results and Discussion

1. Simultaneous Chain- and Step-Growth Radical Polymerization of MA and 1. An equimolar mixture of MA and **1** was copolymerized with CuCl/HMTETA in toluene at 80 °C. Both monomers were simultaneously and quantitatively consumed, in which the consumption of MA was slightly faster than that of **1** (Figure 1A). In addition to the gas-chromatographic analysis of the monomer conversions, the consumption of the original C−Cl and unconjugated C═C bonds was measured by ^{1}H NMR analysis of the reaction mixture to clarify the polymerization mechanism. The original C−Cl bond (filled triangles in Figure 1A) was more rapidly consumed than the unconjugated C═C bond (open triangles), suggesting that the C−Cl bond was first activated by the copper catalyst to form the radical species followed by the addition of the C═C bonds of MA or **1**. The molecular weight of the copolymers was

---

(12) Kato, M.; Kamigaito, M.; Sawamoto, M.; Higashimura, T. *Macromolecules* **1995**, *28*, 1721–1723.

(13) Wang, J.-S.; Matyjaszewski, K. *J. Am. Chem. Soc.* **1995**, *117*, 5614–5615.

(14) Percec, V.; Barboiu, B. *Macromolecules* **1995**, *28*, 7970–7972.

(15) Patten, T. E.; Xia, J.; Abernathy, T.; Matyjaszewski, K. *Science* **1996**, *272*, 866–868.

(16) Granel, C.; Dubois, Ph.; Jérôme, R.; Teyssié, Ph. *Macromolecules* **1996**, *29*, 8576.

(17) Haddleton, D. M.; Jasieczek, C. B.; Hannon, M. J.; Shooter, A. J. *Macromolecules* **1997**, *30*, 2190.

(18) Matyjaszewski, K.; Xia, J. *Chem. Rev.* **2001**, *101*, 2921–2990.

(19) Kamigaito, M.; Ando, T.; Sawamoto, M. *Chem. Rev.* **2001**, *101*, 3689–3746.

(20) Kamigaito, M.; Ando, T.; Sawamoto, M. *Chem. Rec.* **2004**, *4*, 159–175.

(21) Tsarevsky, N. V.; Matyjaszewski, K. *Chem. Rev.* **2007**, *107*, 2270–2299.

(22) Braunecker, W. A.; Matyjaszewski, K. *Prog. Polym. Sci.* **2007**, *32*, 93–146.

(23) Matyjaszewski, K.; Tsarevsky, N. V. *Nat. Chem.* **2009**, *1*, 276–288.

(24) Ouchi, M.; Terashima, T.; Sawamoto, M. *Chem. Rev.* **2009**, *109*, 4963–5050.

(25) Rosen, B. M.; Percec, V. *Chem. Rev.* **2009**, *109*, 5069–5119.

(26) Satoh, K.; Mizutani, M.; Kamigaito, M. *Chem. Commun.* **2007**, 1260–1262.

(27) Mizutani, M.; Satoh, K.; Kamigaito, M. *Macromolecules* **2009**, *42*, 472–480.

(28) Satoh, K.; Ozawa, S.; Mizutani, M.; Nagai, K.; Kamigaito, M. *Nat. Commun.* **2010**, *1*, 6.

(29) Monomers possessing a conjugated C═C and reactive C−X bonds, coined inimers, undergo self-condensing vinyl polymerization to result in hyperbranched polymers; (a) Fréchet, J. M. J.; Henmi, M.; Gitsov, I.; Aoshima, S.; Leduc, M. R.; Grubbs, R. B. *Science* **1995**, *269*, 1080–1083. (b) Litvinenko, G. I.; Simon, P. F. W.; Müller, A. H. E. *Macromolecules* **1999**, *32*, 2410–2419.

(30) Recently, the metal-catalyzed radical forming reaction from organic halides was evolved into step-growth polycondensation of dihalides via atom transfer radical coupling reactions; Durmaz, Y. Y.; Aydogan, B.; Cianga, I.; Yagci, Y. *ACS Symp. Ser.* **2009**, *1023*, 171–187.

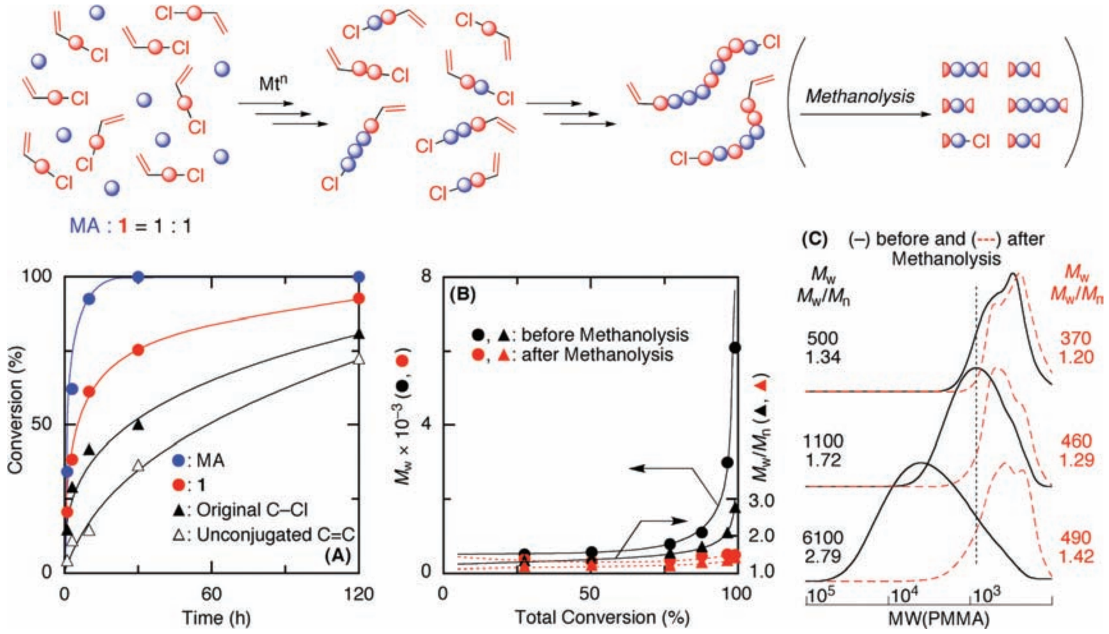

Figure 1. Simultaneous radical chain- and step-growth polymerization of MA and **1** with CuCl/HMTETA in toluene at 80 °C: $[MA]_0 = 2.0$ M; $[\mathbf{1}]_0 = 2.0$ M; $[CuCl]_0 = 100$ mM; $[HMTETA]_0 = 100$ mM. (A) Consumption of MA and **1** measured by gas chromatography and C−Cl and C=C bonds measured by ^{1}H NMR. (B) M_w and M_w/M_n values of the obtained copolymers vs total monomer conversion of MA and **1**. (C) Size-exclusion chromatograms of the obtained copolymers (solid lines) and the methanolyzed products (red dashed lines).

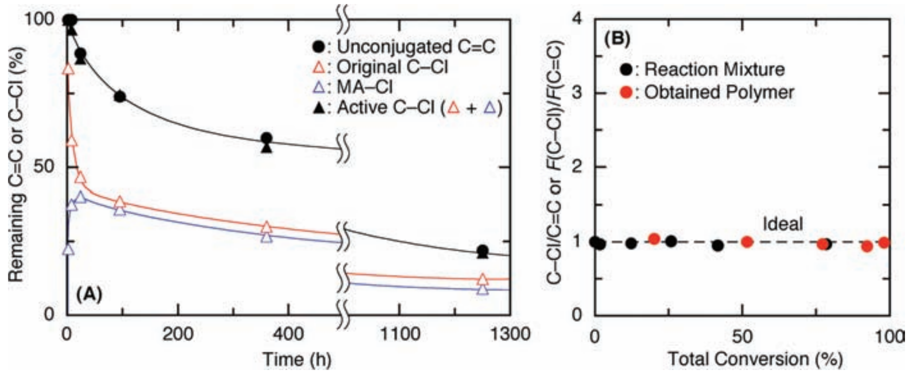

Figure 2. Simultaneous radical chain- and step-growth polymerization of MA and **1** with CuCl/HMTETA in toluene at 60 °C: $[MA]_0 = 2.0$ M; $[\mathbf{1}]_0 = 2.0$ M; $[CuCl]_0 = 100$ mM; $[HMTETA]_0 = 100$ mM. (A) Concentration of remaining unconjugated C=C, original C−Cl, MA−Cl, and sum of the active C−Cl (original C−Cl + MA−Cl) bonds in the reaction mixture measured by ^{1}H NMR. (B) Remaining C−Cl/C=C in the reaction mixture vs total conversion of active C−Cl and unconjugated C=C or F(C−Cl)/F(C=C) values of the obtained polymers after purification vs total monomer conversion of MA and **1**.

relatively low during the initial stage of the polymerizations and progressively increased in the later stage (filled black circles in Figure 1B). The size-exclusion chromatograms (SEC) of the obtained products drastically shifted to higher molecular weights especially in the later stage of the polymerization (bold black curves in Figure 1C), indicating contribution of the step-growth propagation to the product formation.[27]

As we have already reported for the metal-catalyzed step-growth radical homopolymerization of **1**, one of the criteria for the ideal step-growth radical polymerization without side reactions is an equal consumption rate or equal remaining concentration of the active C−Cl and unconjugated C=C bonds during the polymerization.[27] Similarly, even for the ideal simultaneous polymerization of MA and **1**, the amount of the remaining unconjugated C=C bonds in the reaction mixture should be the same as the sum of the remaining original C−Cl bonds and another type of active C−Cl bonds formed via the MA addition. Thus, we further measured the concentration of the active C−Cl bonds derived from MA as well as those of the original C−Cl and unconjugated C=C bonds, which exist in the remaining monomer **1** or at the chain end of the reacted monomer **1** unit, by ^{1}H NMR analysis of the reaction mixture (Figure 2A). The methine proton of the active −CH−Cl (−MA−Cl) bond derived from MA can be distinguished from that of the original −CH-Cl of the **1** unit due to the different chemical shifts irrespective of very similar chemical structures (Figure S1 in Supporting Information). The concentrations of these C−Cl and unconjugated C=C groups were determined from the peak areas in comparison to the signals of toluene (solvent) as the internal standard, where their initial concentrations were set at 100%.

Along with a drastic decrease in the original C−Cl (open red triangles in Figure 2A) during the very early stage of the polymerization, the amount of the −MA−Cl abruptly increased (open blue triangles). This indicates that the radical species generated by the cleavage of the active C−Cl in **1** mainly added to the conjugated C=C double bond of MA to form the −MA−Cl terminal. Thus, radical addition to MA predominates

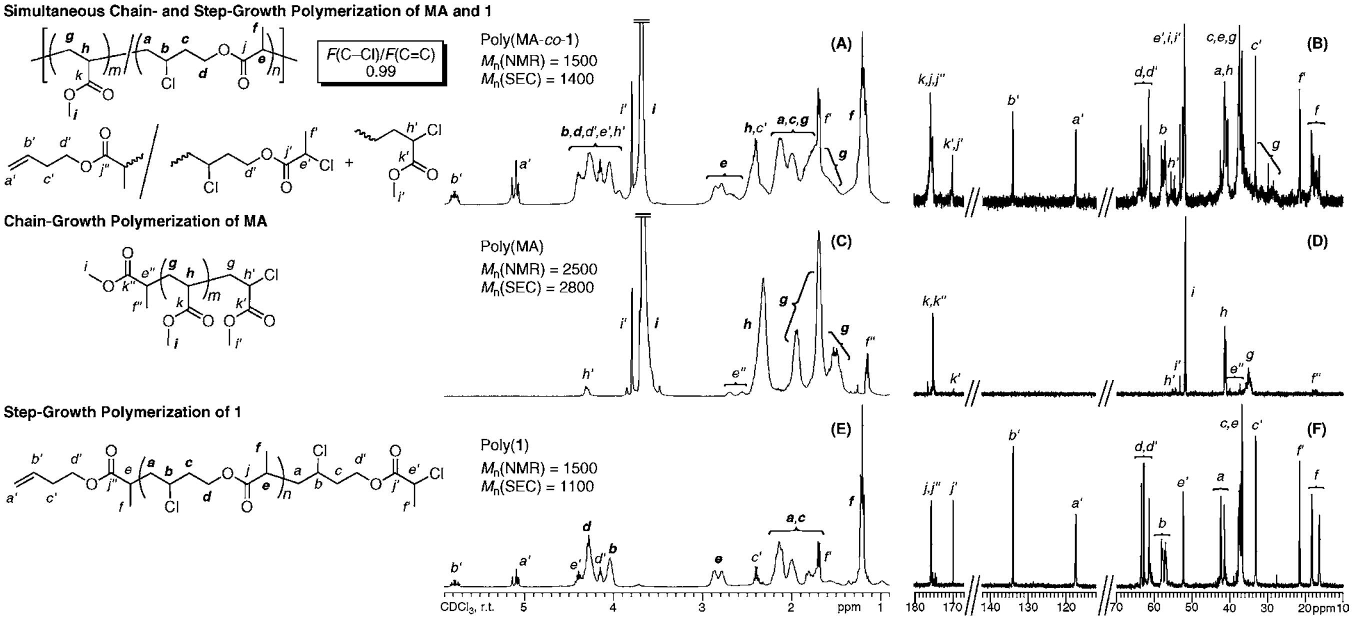

Figure 3. (A) ^{1}H and (B) ^{13}C NMR spectra of poly(MA-*co*-**1**) obtained with CuCl/HMTETA in toluene at 60 °C; (C) ^{1}H and (D) ^{13}C NMR spectra of poly(MA) obtained with RuCp*Cl(PPh$_3$)$_2$ in toluene at 80 °C; (E) ^{1}H and (F) ^{13}C NMR spectra of poly(**1**) obtained with FeCl$_2$/P*n*Bu$_3$ in toluene at 100 °C (CDCl$_3$, r.t.).

in the very early stage. However, sooner or later, both concentrations of the original C−Cl and −MA−Cl simultaneously decreased at similar rates, suggesting that the reactivities of both C−Cl bonds are almost the same. Furthermore, the sum of the remaining concentrations of these active C−Cl bonds (filled black triangles) decreased at the same rate as that of the unconjugated C═C bonds (filled black circles). The ratios of the active C−Cl to the unconjugated C═C bonds (C−Cl/C═C) in the reaction mixture were plotted versus the total conversions of these functional groups (active C−Cl and unconjugated C═C) in Figure 2B (filled black circles) and proved nearly constant around 1.0, indicating the 1:1 reaction requirement for the ideal simultaneous radical polymerizations without side reactions.

The structure of the obtained copolymer was analyzed by ^{1}H and ^{13}C NMR after purification by preparative SEC to remove the residual monomers and catalysts. The ^{1}H and ^{13}C NMR spectra of the obtained products (Figure 3, panels A and B, respectively) principally showed the combined signals of both the homopoly (MA) (Figure 3C,D) and homopoly (**1**) (Figure 3E,F).[27] However, the main-chain signals of each monomer unit (*b*, *d*, *e*, *f*, and *g* in ^{1}H NMR; *b*, *f*, and *g* in ^{13}C NMR) were relatively broad when compared to those of the homopolymers. This suggests that MA and **1** were randomly copolymerized via the chain- and step-growth mechanism, respectively. Furthermore, in the ^{1}H NMR spectrum of the products, almost the same amounts of the unconjugated C═C (*a′*) at the α-end and the active C−Cl (estimated from *i′* and *f′*) at the ω-end were observed [F(C−Cl)/F(C═C) = 0.99]. The number-average molecular weight (M_n) calculated from the terminal to the main-chain protons [M_n (NMR) = 1500] was almost the same as that obtained by size-exclusion chromatography [M_n (SEC) = 1400].

The ratios of the active C−Cl to the unconjugated C═C bonds at the polymer terminals for the copolymer samples obtained at different monomer conversions were also plotted versus the gas-chromatographic total monomer conversions in Figure 2B (filled red circles). The ratios were similarly close to unity during the entire course of the reactions. These results indicated that linear random copolymers of vinyl polymers [poly(MA)] and polyesters [poly(**1**)] without branching were obtained via almost ideal simultaneous metal-catalyzed chain- and step-growth polymerizations.

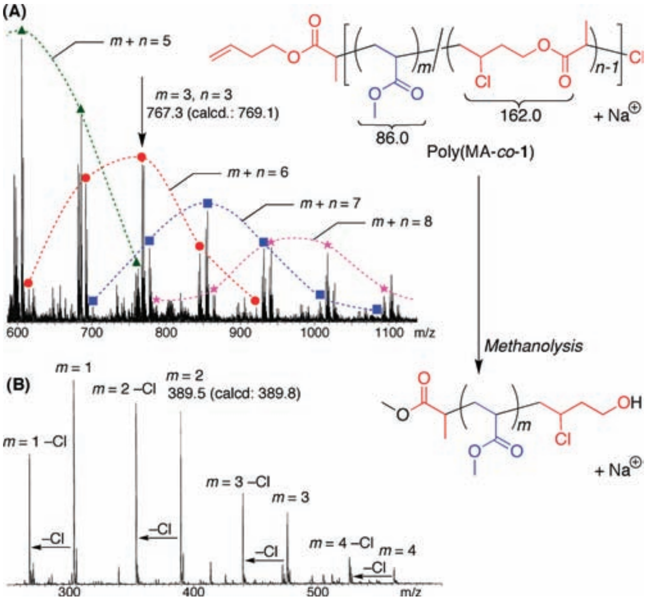

Figure 4. MALDI-TOF-MS spectra of (A) poly(MA-*co*-**1**) (M_n = 1200, M_w/M_n = 2.28) obtained with CuCl/HMTETA: [MA]$_0$ = 2.0 M; [**1**]$_0$ = 2.0 M; [CuCl]$_0$ = 100 mM; [HMTETA]$_0$ = 100 mM in toluene at 80 °C and (B) the methanolyzed product (M_n = 340, M_w/M_n = 1.42).

The sequence distribution of each monomer unit in the copolymers was analyzed by MALDI-TOF-MS. The polymers obtained at a 96% total monomer conversion showed a series of peaks, which were separated by the formula weights of each monomer unit (86.0 for MA and 162.0 for **1**) (Figure 4A). For example, a series of peaks of the 6-mers ($m + n = 6$; red circles) consist of the highest peak of 3-units of MA ($m = 3$) and the 3-units of **1** ($n = 3$) and lower populations of other combinations [(m,n) = (5,1), (4,2), (2,4), (1,5)], indicating that each monomer unit was randomly distributed in the main chains.

Table 1. Metal-Catalyzed Simultaneous Chain- and Step-Growth Radical Polymerization of MA and **1**

		[Monomer]$_0$, M				monomer conv., %^{b}					
entry	metal catalyst^a	MA	**1**	temp., °C	time, h	MA	**1**	M_w^{c}	M_w/M_n^{c}	MA/**1**^{d}	F(C−Cl)/F(C=C)^d
1	CuCl/HMTETA	2.0	2.0	60	1250	>99	96	3300	2.17	49/51	0.99
2	CuCl/HMTETA	2.0	2.0	80	120	>99	93	3000	2.10	52/48	1.17
3	CuCl/HMTETA^g	2.0	2.0	80	80	92	56	880	1.54	61/39	1.05
4	CuCl/HMTETA	2.0	2.0	100	25	>99	85	2100	2.26	56/44	1.43
5	CuCl/Me$_6$TREN	2.0	2.0	80	24	>99	50	1800	1.94	58/42	1.95
6	CuCl/PMDETA	2.0	2.0	80	600	>99	86	2100	1.99	56/44	1.43
7	CuCl/CuCl$_2$/PMDETA^e	2.0	2.0	80	30	84	46	870	1.60	64/36	1.47
8	FeCl$_2$/PnBu$_3$	2.0	2.0	80	24	52	13	11000	2.67	81/19	3.42
9	FeCl$_3$/PnBu$_3$	2.0	2.0	80	30	69	14	9600	3.23	81/19	3.52
10	RuCp*Cl(PPh$_3$)$_2$^{f}	2.0	2.0	80	1800	84	51	810	1.47	57/43	1.05
11	CuCl/HMTETA	3.0	1.0	80	30	98	87	1600	1.64	76/24	1.06
12	CuCl/HMTETA	3.5	0.5	80	30	95	95	2400	1.82	87/13	1.04
13	CuCl/HMTETA	3.8	0.2	80	200	>99	>99	5100	1.70	94/6	0.95
14	CuCl/HMTETA	3.9	0.1	80	100	91	>99	7100	1.60	97/3	1.06
15	CuCl/HMTETA	4.0	0.04	80	80	79	>99	10900	1.38	99/1	0.95
16	CuCl/HMTETA	10.0	0.1	80	10	97	>99	20700	1.68	99/1	1.05
17	RuCp*Cl(PPh$_3$)$_2$^{f}	3.0	1.0	80	600	96	87	1500	1.82	79/21	1.01
18	RuCp*Cl(PPh$_3$)$_2$^{f}	3.5	0.5	80	120	98	96	3000	1.81	85/15	0.93
19	RuCp*Cl(PPh$_3$)$_2$^{f}	3.9	0.1	80	80	84	>99	6100	1.47	96/4	1.01
20	RuCp*Cl(PPh$_3$)$_2$^{f}	4.0	0.04	80	200	98	>99	18200	1.86	99/1	1.09
21	RuCp*Cl(PPh$_3$)$_2$^{f}	6.0	0.06	80	360	>99	>99	35700	2.01	99/1	1.05

[a] [CuCl]$_0$ = 100 mM, [FeCl$_2$]$_0$ = 20 mM, [FeCl$_3$]$_0$ = 20 mM, [RuCp*Cl(PPh$_3$)$_2$]$_0$ = 4.0 mM, [1,1,4,7,10,10-hexamethyltriethylenetetramine (HMTETA)]$_0$ = 100 mM, [tris[2-(dimethylamino)ethyl]amine (Me$_6$TREN)]$_0$ = 100 mM, [*N*,*N*,*N*′,*N*′′,*N*′′-pentamethyldiethylenetriamine (PMDETA)]$_0$ = 100 mM, [tri*n*-butylphosphine (P*n*Bu$_3$)]$_0$ = 40 mM, in toluene. [b] Determined by gas chromatography. [c] The weight-average molecular weight (M_w) and distribution (M_w/M_n) were determined by size-exclusion chromatography. [d] Determined by ^{1}H NMR. [e] [CuCl]$_0$ = 50 mM, [CuCl$_2$]$_0$ = 50 mM. [f] [nBu$_3$N]$_0$ = 40 mM. [g] [CuCl]$_0$ = 20 mM, [HMTETA]$_0$ = 20 mM

To further examine the random sequence, the copolymers obtained at various monomer conversions were methanolyzed by the cleavage of the main-chain ester linkage originating from **1** to generate the lower molecular weight oligomers as shown by the red dashed SEC curves in Figure 1C. All the molecular weights of the methanolyzed products were around 300−500 (Figure 1C and red filled circles in Figure 1B) and became slightly higher with the total monomer conversion, suggesting that the chain lengths of successive MA units sandwiched between the **1** units were nearly independent of the conversion.

The MALDI-TOF-MS spectrum of the methanolyzed products showed a series of low molecular weight oligomers of MA possessing the cleaved units (methyl propionate and 3-chlorobutyl alcohol units) of **1** at both terminals, in which the unimer and dimer (m = 1 and 2) of MA are predominant with lower amounts of higher mass oligomers (Figure 4B). A series of lower mass peaks (around 36) for each oligomer can be attributed to the loss of the pendent chlorine atom during the laser irradiation. These results indicate that the most probable number of the sequenced-MA units within the copolymers is around 1 to 2 and that MA sequences were randomly separated by the ester-linkages of **1** via the random copolymerizations. The random incorporation of **1** and MA units might seem strange when only considering the double-bond reactivity, which is lower for the unconjugated C=C double bond of **1** than that of the conjugated counterpart of MA. However, it is a natural consequence because **1** is consumed faster as an initiator for the MA polymerization than as a monomer via activation of the C−Cl bond having a similar reactivity of the derived dormant MA terminal that results in short oligomers possessing the unconjugated C=C bond at the other terminal. The short oligomers can be copolymerized with the remaining MA or **1** or other oligomers to produce longer polymer chain, in which the two monomer units were randomly distributed.

The CuCl/HMTETA-catalyzed simultaneous chain- and step-growth polymerization is assumed to proceed by essentially the same secondary carbon-centered growing radical species adjacent to the carbonyl groups originating from MA or **1** as outlined in Scheme 1. The radical species is thus generated by the metal-catalyzed reversible activation of the reactive C−Cl bond adjacent to C=O and then adds to either of the C=C double bonds in MA or **1**. When the radical adds to MA (path A), the newly generated carbon radical species is similar to the original one and will generate a similarly active C−Cl bond adjacent to the carbonyl group via capping with the chlorine atom. The C−Cl bond can thus be activated again to induce chain-growth propagation. Meanwhile, the addition to **1** results in an unconjugated radical species (path B), which is then capped with chlorine to lead to the inactive C−Cl bond without adjacent carbonyl groups. In contrast, the C−Cl bond originating from the added **1** unit at the terminal can be activated to undergo step-growth propagation. The paths A and B give vinyl polymer and polyester structures, respectively, and thus, the simultaneous copolymerizations lead to their random copolymers. The oligomers or polymers possessing the C=C terminals originating from **1** also react with the growing radical species via path B to induce a drastic molecular weight increase especially at the later stage of the polymerizations.

Although the results described above induced the almost ideal simultaneous radical polymerization under appropriate conditions, there are some possible side reactions, such as the bimolecular radical termination (path C) and chain-growth copolymerization of **1** with MA (path D) depending on the conditions. Before these possibilities with the CuCl/HMTETA system were examined in more detail by analyzing the model reactions (see the next section), other transition metal catalysts, which are effective for the living radical polymerization of acrylates, were used for the copolymerization of MA and **1** at the 1:1 feed ratio under various conditions at different temperatures and with different catalyst concentrations.

All the catalytic systems we examined induced the simultaneous consumptions of MA and **1**, as summarized in Table 1 (entries 1−10) and Figures S2−S5 in Supporting Information, while the activities, conversions, molecular weights, and composition ratios were dependent on the metals, ligands, and conditions. Among these, the FeCl$_2$/PnBu$_3$ system (entry 8 and Figure S4) gave relatively high molecular weight polymers even at low monomer conversions, in which the consumption of MA was much faster than that of **1**, and resulted in decreased molecular weights with the increasing conversions. Furthermore, the content of the active C−Cl bond in the polymer was much higher than that of the C═C bond [F(C−Cl)/F(C═C) = 3.42] (entry 8 and Figure S6E). These results indicate that the chlorine-capping of the carbon radical species derived from **1** was not sufficiently fast using the iron catalyst. Thus, the radical species underwent the addition of MA before the Cl-capping to form the pendent active C−Cl groups originating from the unit **1** that was copolymerized not via the step- but via the chain-growth mechanism (path D in Scheme 1). A similar higher content of the active C−Cl bonds was obtained even with CuCl in the presence of different ligands, such as tris[2-(dimethylamino)-ethyl]amine (Me$_6$TREN) [F(C−Cl)/F(C═C) = 1.95] (entry 5; Figures S2 and S6D) and *N*,*N*,*N*′,*N*″,*N*″-pentamethyldiethylenetriamine (PMDETA) [F(C−Cl)/F(C═C) = 1.43] (entry 6; Figures S3 and S6C), while the values were lower than that with FeCl$_2$/PnBu$_3$. A higher oxidation metal species, such as FeCl$_3$ (entry 9) or CuCl$_2$ (entry 7), was also employed for the purpose of enhancing the capping reaction, but resulted in having almost no effect on lowering the F(C−Cl)/F(C═C) values. Even for the CuCl/HMTETA system, the F(C−Cl)/F(C═C) ratio slightly deviated from 1.0 upon increasing the temperature (entries 2 and 4). However, by lowering the metal-catalyst concentration, the value became close to unity even at the same temperature (entry 3). Another good metal catalyst candidate proved to be RuCp*Cl(PPh$_3$)$_2$, which gave an almost equal content of the remaining active C−Cl and unconjugated C═C bonds in the copolymer (entry 10; Figure S6B), although the reaction was very slow to produce lower molecular weight oligomers (Figure S5). We should now note how the F(C−Cl)/F(C═C) values reflect the obtained copolymer structures. For example, F(C−Cl)/F(C═C) = 1.10 means that 90% of the obtained copolymers are linear without any pendent or branching active C−Cl bonds and that the remaining 10% are copolymers with only one pendent active C−Cl unit in the polymer chain on average. As another example, F(C−Cl)/F(C═C) = 2.0 means that the copolymers have one pendent or branching structure per chain on average. Therefore, most of the copolymers obtained using copper and ruthenium catalysts have nearly linear structures without significant branching.

Thus, the choice of the catalyst as well as the reaction conditions is important for the ideal metal-catalyzed chain- and step-growth radical polymerizations so that the catalyst should induce a fast halogen capping for generating polyester structures from **1** as well as fast polymerization for giving higher molecular weight products. Among the various catalysts we investigated, the CuCl/HMTETA system proved most effective in giving the linear copolymers via almost ideal simultaneous chain- and step-growth radical polymerizations under the appropriate conditions (entries 1 and 3).

2. Model Reactions for Detailed Analysis of Simultaneous Radical Polymerization. 2.1. Model Reaction for Estimating the Possible Bimolecular Radical Reactions (Path C). To reveal the effects of possible side reactions, especially the bimolecular termination between the radical species, we first investigated the metal-catalyzed Kharasch radical addition or ATRA between methyl 2-chlroropropionate (**2**) and 3-butenyl acetate (**3**), which can be regarded as model compounds of the active C−Cl and unconjugated C═C bonds of **1**, respectively, by using various metal catalysts (Scheme 2).[27]

Scheme 2. Model Reaction between **2** (C−Cl Bond of **1**) and **3** (C═C Bond of **1**) in the Absence of MA

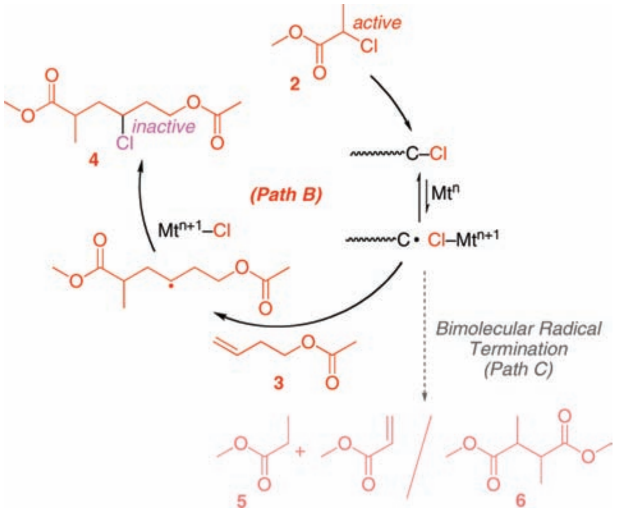

Figure 5A shows the conversions of the chloride (**2**) and vinyl (**3**) compounds (filled red circles and triangles, respectively) in the CuCl/HMTETA-catalyzed radical addition at 80 °C. Both model compounds were simultaneously consumed at the same rate to almost quantitatively produce the adduct (**4**). Furthermore, the consumption rates were almost the same as those of the active C−Cl (open black circles) and the unconjugated C═C (open black triangles) for the polymerization under the same conditions (cf. Figure 1A), suggesting a good model reaction for the simultaneous polymerization.

The ^{1}H NMR analysis of the reaction mixture also revealed that the yield of the adduct (**4**) was almost the same for the conversion of **2** or **3** and that more than 99% of the reacted **2** and **3** were thus converted into **4** without any significant formation of byproducts (entry 1 in Table S1). A further detailed gas-chromatographic analysis of the reaction mixture showed the minimal formation (1%) of methyl propionate (**5**), which formed via disproportionation of the radical species derived from **2**, and no coupling product [dimethyl 2,3-dimethyl succinate (**6**)] of the radical (Figure 5B and entry 1 in Table S1). In addition, the product obtained after purification by column chromatography followed by evaporation of the volatile compounds (**2**, **3**, **5**, and toluene) proved exclusively to be the adduct (**4**) without contamination by any byproducts, which might be formed via a bimolecular radical termination originating from the adduct radical. These results indicate that CuCl/HMTETA induced an almost ideal radical addition between **2** and **3** to give **4**. Similar results were obtained with CuCl/Me$_6$TREN or reported[27] with CuCl/PMDETA, RuCp*Cl(PPh$_3$)$_2$, and FeCl$_2$/PnBu$_3$, in which a high yield of the adduct was attained without significant bimolecular radical termination, while the contents slightly depended on the catalytic systems (Table S1).

2.2. Model Reactions for Estimating the Possible Chain-Growth Radical Copolymerization of 1 with MA (Path D). To estimate the contribution of the possible chain-growth radical copolymerization of **1** with MA affording the pendent active C−Cl bonds in the copolymer chains, we investigated the radical addition and/or possible polymerization of **3**, a model of the unconjugated C═C bond of **1**, and MA

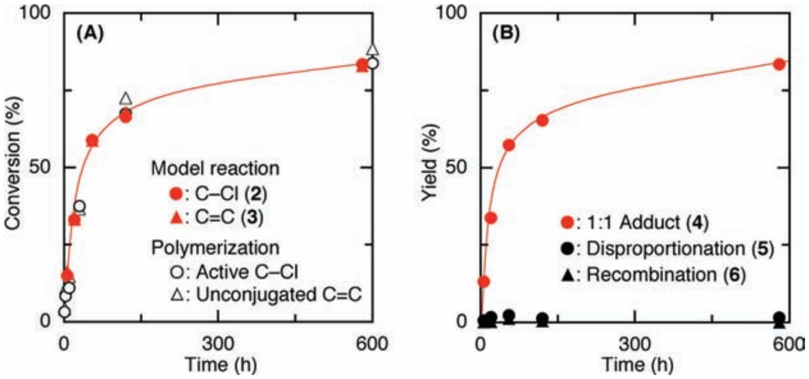

Figure 5. Model reaction of **2** and **3** with CuCl/HMTETA in the absence of MA in toluene at 80 °C: $[\mathbf{2}]_0 = 2.0$ M; $[\mathbf{3}]_0 = 2.0$ M; $[\mathrm{CuCl}]_0 = 100$ mM; $[\mathrm{HMTETA}]_0 = 100$ mM. (A) Consumption of **2** and **3** (solid lines) in the model reaction and active C−Cl and unconjugated C═C bonds in the polymerization of MA and **1** measured by ^{1}H NMR. (B) Yield of **4** measured by ^{1}H NMR and **5** and **6** measured by gas chromatography.

Scheme 3. Model Reaction between **2** (C−Cl Bond of **1**) and **3** (C═C Bond of **1**) in the Presence of MA

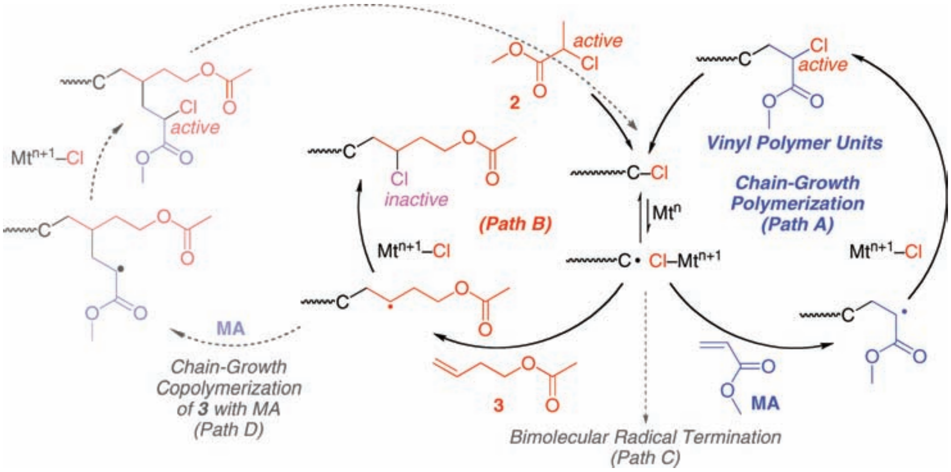

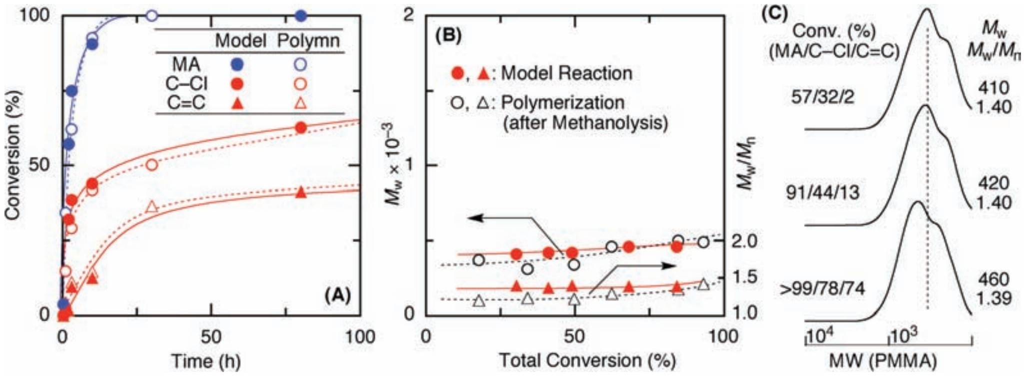

Figure 6. Model reaction of **2** and **3** with CuCl/HMTETA in the presence of MA in toluene at 80 °C: $[\mathbf{2}]_0 = 2.0$ M; $[\mathbf{3}]_0 = 2.0$ M; $[\mathrm{MA}]_0 = 2.0$ M; $[\mathrm{CuCl}]_0 = 100$ mM; $[\mathrm{HMTETA}]_0 = 100$ mM. (A) Consumption of MA, **2**, and **3** (solid lines) in the model reaction and MA, original C−Cl, and unconjugated C═C bonds in the polymerization of MA and **1** (dashed lines) measured by ^{1}H NMR. (B) M_w and M_w/M_n values of the obtained oligomers in the model reaction vs total conversion of MA, **2**, and **3** (solid lines) and the methanolyzed products of the copolymers obtained in the polymerization of MA and **1** (dashed lines). (C) Size-exclusion chromatograms of the obtained oligomers in the model reaction.

with **2**, a model of the active C−Cl bond of **1**, under the equimolar concentration ($[\mathbf{2}]_0 = [\mathbf{3}]_0 = [\mathrm{MA}]_0 = 2.0$ M) by using various catalysts in a way similar to the simultaneous polymerization (Scheme 3). Under the conditions that **1** will undergo an ideal step-growth propagation during the simultaneous polymerization, the model compound, **3**, with the unconjugated C═C double bond, but without the active C−Cl bond, should not be incorporated into the main chain, but should be located at the chain end.

Figure 6A shows the consumptions of MA (filled blue circles), **2** (filled red circles), and **3** (filled red triangles) in the model reaction with CuCl/HMTETA at 80 °C. The consumption rates of MA, **2**, and **3** for the model reaction indicated by the three solid curves were in good agreement with those of MA, the original C−Cl, and the unconjugated C═C bonds, respectively, for the simultaneous polymerization indicated by the three dashed curves. This also shows a good model reaction for the simultaneous polymerization.

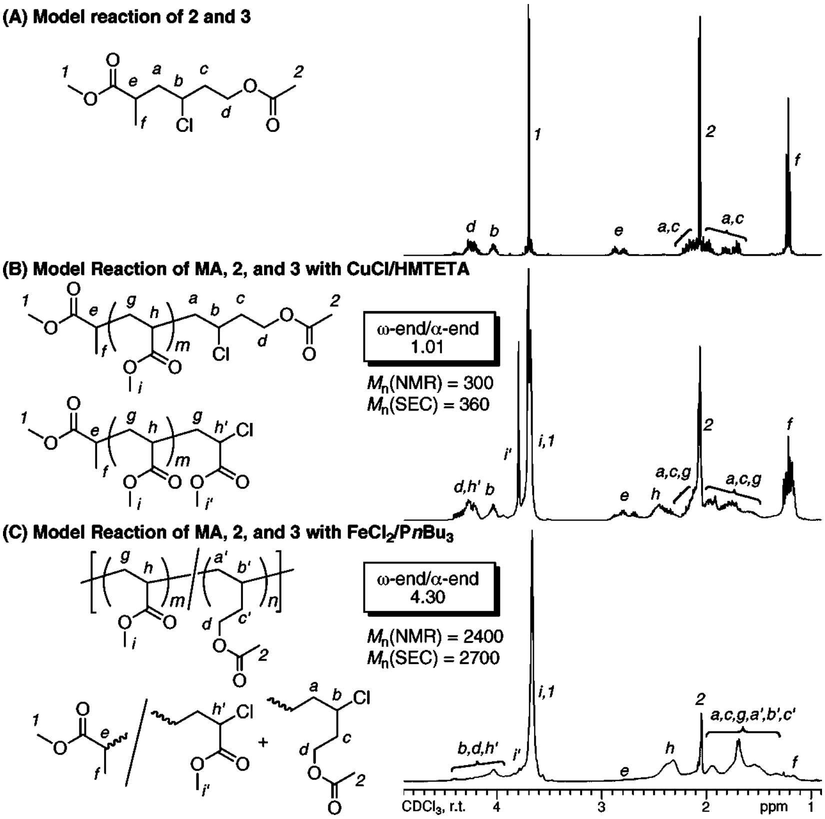

Figure 7. ^{1}H NMR spectra of (A) **4** and the oligomer obtained in the model reaction of **2**, **3**, and MA with (B) CuCl/HMTETA and (C) $FeCl_2/PnBu_3$ in toluene at 80 °C ($CDCl_3$, r.t.).

The molecular weights of the obtained products were low ($M_w \sim 400$) and increased very slightly with the total conversion of these compounds (filled circles in Figure 6B). The molecular weights, molecular weight distributions (filled triangles), and SEC curves (Figure 6C) were quite similar to those of the products obtained by methanolysis of the copolymers in the simultaneous polymerization (open circles and triangles in Figure 6B; cf. panels B and C in Figure 1). These results suggest that the model reaction induced oligomerization of MA via activation of the C−Cl bond of **2** with CuCl/HMTETA and the chain-propagation was irreversibly terminated sooner or later by the addition of the C═C bond of **3**.

Other metal catalysts, such as CuCl/Me_6TREN, CuCl/PMDETA, and RuCp*Cl$(PPh_3)_2$, induced the simultaneous consumption, in which the rates were dependent on the catalysts and principally resulted in similar oligomers in terms of what can be observed in the SEC analysis while the molecular weights were slightly higher than that with CuCl/HMTETA (Figures S7, S8, and S10 in Supporting Information). In contrast, the $FeCl_2/PnBu_3$ system induced a much faster MA consumption than **2** and **3** to afford high molecular weight polymers (Figure S9 in Supporting Information) in a similar manner to the copolymerization of MA and **1** (Figure S4). Furthermore, the C═C model compound (**3**) was consumed faster than the C−Cl counterpart (**2**), suggesting that chain-growth copolymerization of **3** might occur in the $FeCl_2/PnBu_3$ system.

The structures of the products obtained in the 1:1:1 model reactions of **2**, **3**, and MA with various metal catalysts were analyzed by ^{1}H NMR and MALDI-TOF-MS. The product obtained with CuCl/HMTETA (Figure 7B) showed several similar signals to those (*1*, *2*, *a*−*f* in Figure 7A) of the 1:1 adduct (**4**) of **2** and **3**. In addition to these, signals originating from the MA units (*g*, *h*, *i*, *h′*, and *i′*) were observed. These results suggests that the following consecutive reactions occurred: The radical addition or polymerization of MA was first initiated from **2** (α-end), and some of the radical species were capped with **3** resulting in the inactive C−Cl terminal at the *ω*-end, while a part of the *ω*-ends was not capped with **3** and was still the active C−Cl terminal originating from MA. More importantly, **3** was not incorporated in the main chain, but located at the chain end, which was indicated by the fact that the ratio of the *ω*-end groups, that is, sum of the acetyl signal (*2*) of **3** and the MA terminal (*i′*), to the α-end, that is, the methyl group (*f*) of **2**, was close to unity (*ω*-end/α-end = 1.01). These results indicated that the chain-growth cross-propagation of the radical species derived from **3** to MA is negligible with CuCl/HMTETA under the appropriate conditions. A similar result was also obtained with RuCp*Cl$(PPh_3)_2$ (*ω*-end/α-end = 1.00; Figure S13 in Supporting Information).

On the other hand, $FeCl_2/PnBu_3$ gave a higher content of *ω*-ends than α-ends (*ω*-end/α-end = 4.30; Figure 7C), indicating that the chain-growth radical copolymerization of **3** with MA occurred to give the pendent acetyl moieties originating from **3** in the copolymers. A similar higher content of the *ω*-ends was observed with CuCl/PMDETA (*ω*-end/α-end = 1.27; Figure S13B) and CuCl/Me_6TREN (*ω*-end/α-end = 1.32; Figure S13C), while these values were lower than that with $FeCl_2/PnBu_3$. All these *ω*-end/α-end values in the model reactions were similar to those of *F*(C−Cl)/*F*(C═C) obtained during the simultaneous copolymerizations, indicating that these model reaction studies well reflect the copolymerizations.

The MALDI-TOF-MS analysis of the products obtained in the model reactions also gave useful information on the copolymerizations as shown in Figure 8. The MALDI-TOF-

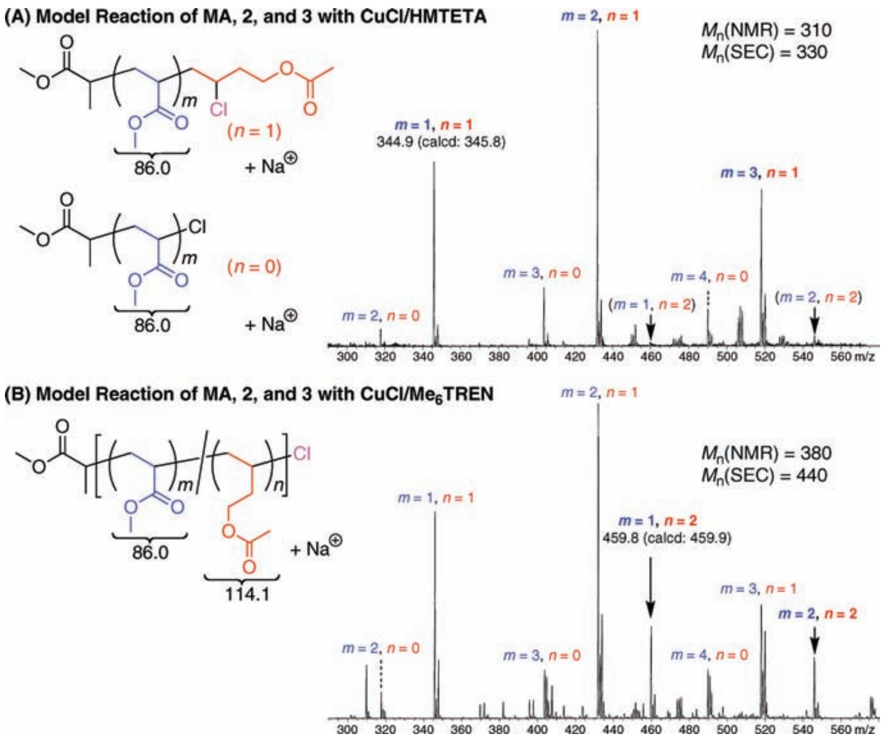

Figure 8. MALDI-TOF-MS spectra of the oligomer obtained in the model reaction of **2**, **3**, and MA with (A) CuCl/HMTETA ($M_n = 330$, $M_w = 490$, $M_w/M_n = 1.48$) and (B) CuCl/Me$_6$TREN in toluene at 80 °C ($M_n = 440$, $M_w = 630$, $M_w/M_n = 1.43$).

MS spectrum of the product obtained with CuCl/HMTETA (Figure 8A) shows a main series of peaks with one unit of **2**, a small number (m) of MA units, and one unit of **3** [(m,n) = (1,1), (2,1), (3,1)]. In addition to these peaks, a minor series of peaks appeared, assignable to the MA oligomers possessing **2** at the α-end and an active −MA−Cl bond at the ω-end [(m,n) = (2,0), (3,0), (4,0)]. In contrast, another possible series of peaks with more than 2 units of **3**, such as (m,n) = (1,2), (2,2), was hardly observed. These results indicate again almost no contribution of the chain-growth radical copolymerization of **3** with MA. A similar MALDI-TOF-MS spectrum was also obtained with RuCp*Cl(PPh$_3$)$_2$ (Figure S14A in Supporting Information).

In contrast, the products obtained with CuCl/Me$_6$TREN (Figure 7B) exhibited a series of peaks possessing 2 units of **3** [(m,n) = (1,2), (2,2)] in addition to two series of peaks with n = 1 and 0, suggesting that the chain-growth radical copolymerization of **3** with MA cannot be ruled out for this catalytic system. The CuCl/PMDETA system gave similar results (Figure S14B in Supporting Information).

These detailed model studies support the fact that the metal-catalyzed simultaneous chain- and step-growth radical copolymerization of MA and **1** is achievable without any significant contribution of side reactions, such as the bimolecular radical termination and chain-growth propagation of **1**, by careful selection of the catalytic systems and the conditions. Among the various catalysts we investigated, the best one proved to be CuCl/HMTETA or RuCp*Cl(PPh$_3$)$_2$, which afforded linear random copolymers of the vinyl monomer and polyester units.

In addition to these findings for the simultaneous polymerizations, the model reaction studies would provide useful information on the metal-catalyzed radical addition copolymerization of acrylate and unconjugated α-olefin, such as propylene and 1-hexene, because the model compound **3** possesses a similar C═C bond to these α-olefins. On the basis of our results in the model reactions, CuCl/HMTETA or RuCp*Cl(PPh$_3$)$_2$ may not be suitable for producing the high molecular weight copolymers while FeCl$_2$/PnBu$_3$ can give relatively high molecular weight copolymers with a small amount of α-olefin units.

3. Synthesis of Various Composition Copolymers: From Multiblock to Random Copolymers. A series of copolymerizations of MA and **1** with different feed ratios ([MA]$_0$/[**1**]$_0$ = 3/1, 7/1, 19/1, 39/1, and 100/1) was then carried out with CuCl/HMTETA or RuCp*Cl(PPh$_3$)$_2$, which were effective for the simultaneous step- and chain-growth radical copolymerizations at the 1/1 monomer feed ratio, as summarized in Table 1 (entries 11−21). In all cases, both monomers were simultaneously consumed. More specifically, when the polymerization was carried out at the 100/1 feed ratio, the C−Cl bond of **1** was consumed faster than MA, as shown in Figure 9A. Furthermore, the consumption rate of the C−Cl bond of **1** was greater than that of the C═C double bond of **1**. These results suggest that most of **1** was consumed via the reaction of the C−Cl bond during the initial stage of the copolymerizations.

The M_n of the products (filled black circles in Figure 9B) increased in almost direct proportion to the total monomer conversion in the initial stage and agreed well with the calculated values assuming that one polymer chain is generated from one molecule of **1**. Furthermore, after the complete consumption of the monomers, the M_n values progressively increased and the SEC curves became multimodal (Figure 9C). These results indicated that the transition metal catalyst first activates the C−Cl bond of **1** to almost exclusively induce the chain-growth living radical polymerization of MA in the initial stage. The metal catalyst then gradually induces the step-growth propagation between the active C−Cl terminal of poly(MA), which was formed by the living chain-polymerization, and the unconjugated C═C double bond at the α-end originating from **1** to give the multiblock polymers consisting of poly(MA) segments connected by the ester linkage of **1**.

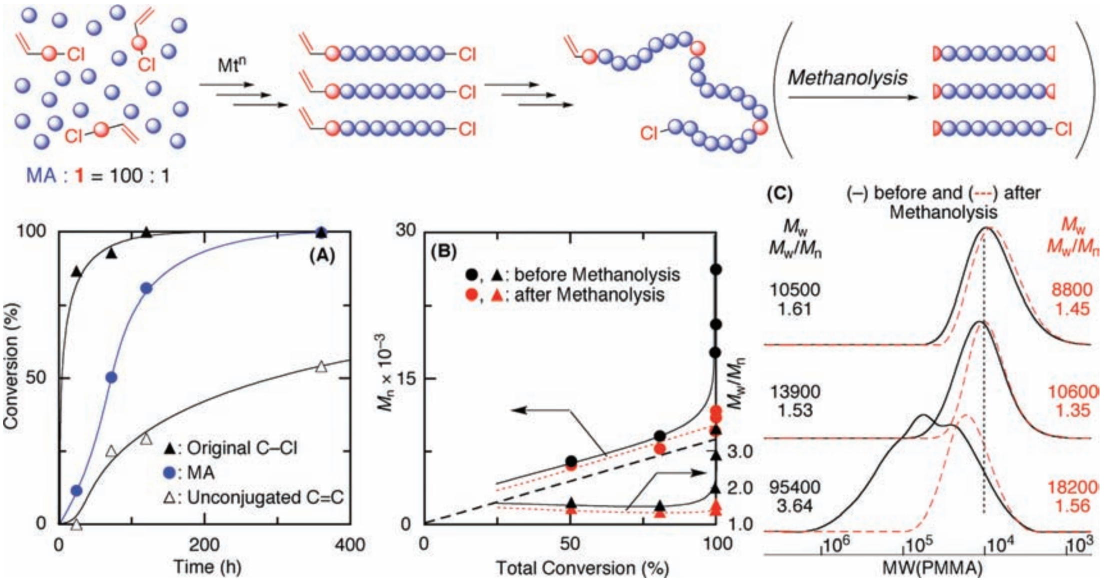

Figure 9. Simultaneous radical chain- and step-growth polymerization of MA and **1** with RuCp*Cl(PPh$_3$)$_2$ in toluene at 80 °C: [MA]$_0$ = 6.0 M; [**1**]$_0$ = 60 mM; [RuCp*Cl(PPh$_3$)$_2$]$_0$ = 4.0 mM; [nBu$_3$N]$_0$ = 40 mM. (A) Consumption of MA measured by gas chromatography and original C−Cl and unconjugated C═C bonds measured by ^{1}H NMR. (B) M_n and M_w/M_n values of the obtained copolymers vs total monomer conversion of MA and **1**. The diagonal black dashed line indicates the calculated M_n assuming the formation of one living polymer of MA per one **1** molecule. (C) Size-exclusion chromatograms of the obtained copolymers (solid lines) and the methanolyzed products (red dashed lines).

These multiblock polymers were then methanolyzed by sodium carbonate which resulted in the unimodal SEC curves (red dashed curves in Figure 9C), and the M_n of which (filled red circles in Figure 9B) was very close to the calculated values for the formation of living polymers from **1**. Thus, the synthesis of a series of copolymers changing from random to multiblock polymer structures was attained by varying the monomer feed ratio of MA to **1** with the appropriate catalysts.

Conclusions

We succeeded in inducing the simultaneous chain- and step-growth radical polymerizations of methyl acrylate and a designed monomer possessing unconjugated C═C and active C−Cl bonds via the same metal-catalyzed reaction to produce a series of novel linear copolymers consisting of vinyl polymer and polyester units. The choice of the catalysts and reaction conditions is crucial for the controlled synthesis of the linear random copolymers without branching structures originating from the unfavorable chain-growth propagation of the designed monomers. By varying the monomer feed ratios, the structures of the obtained copolymers were varied from random to multiblock copolymers having different segment lengths of vinyl monomer units chopped by the polyester units, which can be controlled by the monomer feed ratio. The copolymers thus possess ester linkages in the main chain, which can be degradable to lower molecular weight vinyl polymers or oligomers under the appropriate conditions. This will produce unique properties for the copolymers for certain applications. By using the advantage of the radical polymerization, the incorporation of functional groups between the C═C and C−Cl groups in the designed monomers as well as in the pendent groups of the vinyl monomer is promising for giving functions to the copolymers. We are also expanding the scope to other linear random copolymers, such as those comprised of acrylamide and polyamide units in the main chain. We believe that the simultaneous chain- and step-growth polymerization will provide new strategies for designing novel polymer syntheses.

Acknowledgment. This work was supported in part by a Grant-in-Aid for Young Scientists (S) (No. 19675003) by the Japan Society for the Promotion of Science and the Global COE Program "Elucidation and Design of Materials and Molecular Functions."

Supporting Information Available: Experimental procedures, polymerizations, model reactions, NMR and MALDI-TOF-MS spectra. This material is available free of charge via the Internet at http://pubs.acs.org.

JA1023892